NeuroImage: Clinical 24 (2019) 102071

Contents lists available at ScienceDirect

NeuroImage: Clinical

journal homepage: www.elsevier.com/locate/ynicl

Abnormal dynamic properties of functional connectivity in disorders of consciousness

Bolin Cao[a,1], Yan Chen[b,1], Ronghao Yu[b], Lixiang Chen[a], Ping Chen[a], Yihe Weng[a], Qinyuan Chen[a], Jie Song[a], Qiuyou Xie[c,*], Ruiwang Huang[a,*]

[a] Center for the Study of Applied Psychology and MRI Center, Key Laboratory of Mental Health and Cognitive Science of Guangdong Province, School of Psychology, South China Normal University, Guangzhou 510631, China
[b] Centre for Hyperbaric Oxygen and Neurorehabilitation, Liuhuaqiao Hospital, Guangzhou 510010, China
[c] Department of Rehabilitation Medicine, ZhuJiang Hospital of Southern Medical University, Guangzhou 510280, China

ARTICLE INFO

Keywords:
Independent component analysis (ICA)
Sliding windows approach
Connectome-based predictive model (CPM)
Hidden Markov model (HMM)

ABSTRACT

Resting-state functional magnetic resonance imaging (rs-fMRI) is widely used to research abnormal functional connectivity (FC) in patients with disorders of consciousness (DOC). However, most studies assumed steady spatial-temporal signal interactions between distinct brain regions during the scan period. The aim of this study was to explore abnormal dynamic functional connectivity (dFC) in DOC patients. After excluding 26 patients' data that failed to meet the requirements of imaging quality, we retained 19 DOC patients (12 with unresponsive wakefulness syndrome and 7 in a minimally conscious state, diagnosed with the Coma Recovery Scale-Revised [CRS-R]) for the dFC analysis. We used the sliding windows approach to construct dFC matrices. Then these matrices were clustered into distinct states using the *k*-means clustering algorithm. We found that the DOC patients showed decreased dFC in the sensory and somatomotor networks compared with the healthy controls. There were also significant differences in temporal properties, the mean dwell time (*MDT*) and the number of transitions (*NT*), between the DOC patients and the healthy controls. In addition, we also used a hidden Markov model (HMM) to test the robustness of the results. With the connectome-based predictive modeling (CPM) approach, we found that the properties of abnormal dynamic network can be used to predict the CRS-R scores of the patients after severe brain injury. These findings may contribute to a better understanding of the abnormal brain networks in DOC patients.

1. Introduction

It was nearly impossible to observe overt behavioral response in disorders of consciousness (DOC) patients without the ability to move and/or communicate verbally (Bosco et al., 2010; Schnakers et al., 2009). Using the task-fMRI technique, Owen et al. (2006) acquired fMRI data from a vegetative state/unresponsive wakefulness syndrome (VS/UWS) patient when she was performing the mental imagery tasks (playing tennis and visiting house) and found that the patient showed similar brain activation patterns compared with the healthy control. This study provided critical evidence that consciousness in brain injured people is detectable even the patients are behaviorally non-responsive. Subsequently, Monti et al. (2010) collected fMRI data from 54 DOC patients who performed similar mental imagery tasks, observed that five patients could react to command by generating specific neural responses and two of the five were diagnosed as VS/UWS patients who by definition lack overt behavioral responses. Actually, because the brain injury severity and impaired cognitive ability vary in DOC patients, it is obvious that not all DOC patients could follow verbal or other commands to finish a task-fMRI experiment. As subjects do not need to do any behavioral responses, the rs-fMRI technique is widely adopted to study abnormal brain function and functional connectivity

Abbreviations: DOC, disorders of consciousness; VS/UWS, vegetative state/unresponsive wakefulness syndrome; MCS, minimally conscious state; CRS-R, Coma Recovery Scale-Revised; fMRI, functional magnetic resonance imaging; MNI, Montreal Neurological Institute; FC, functional connectivity; ICA, independent component analysis; IC, independence component; ICN, intrinsic connectivity network; HMM, hidden Markov model; CPM, connectome-based predictive modeling; DMN, default mode network; CCN, cognitive control network; VSN, visual network; AUN, auditory network; CBN, cerebellar network; SMN, somatomotor network; SCN, subcortical network; MDT, mean dwell time; NT, number of transitions; SVM, support vector machine

* Corresponding authors.
E-mail addresses: xqy7180@163.com (Q. Xie), ruiwang.huang@gmail.com (R. Huang).
[1] Both authors contributed equally to this work.

https://doi.org/10.1016/j.nicl.2019.102071
Received 24 June 2019; Received in revised form 9 October 2019; Accepted 4 November 2019
Available online 05 November 2019

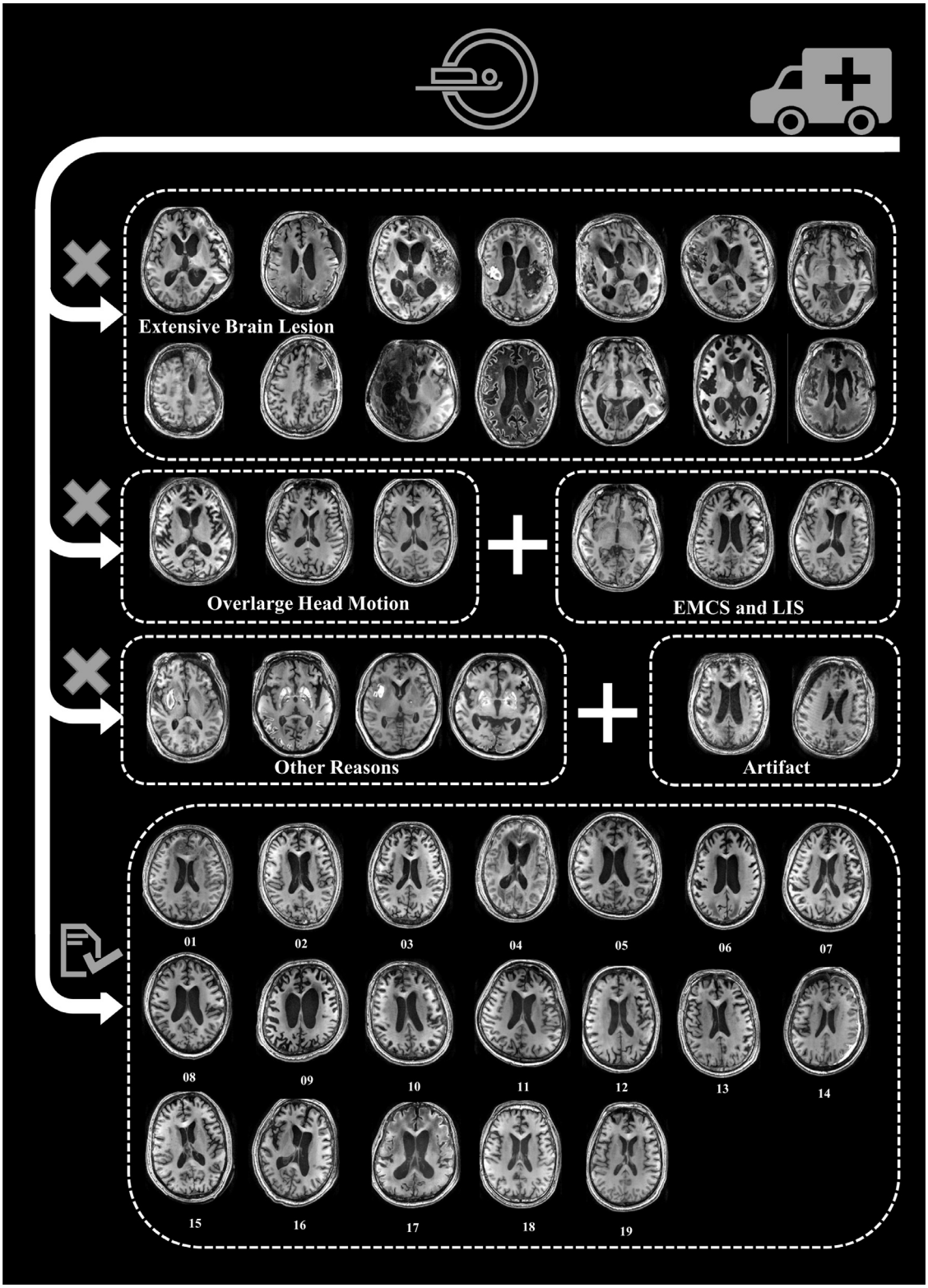

Fig. 1. Illustration of brain structure images for the patients with disorders of consciousness (DOC) showing those included and those excluded. In total, we acquired imaging data (rs-fMRI and high-resolution brain structural images) from 45 patients. In the data analysis, we only included 19 patients in the current study after excluding 26 patients from the total data sample. The imaging data for these 26 patients were excluded because they had at least one of these imaging qualities or clinical conditions: heavy artifact, brain lesion or atrophy, overlarge head motion, diagnosed with LIS (locked-in syndrome) or EMCS (emerged minimally conscious state), and other type imaging quality problems.

(FC) in various brain disorders such as DOC patients (Demertzi et al., 2019; Perri et al., 2016; Hannawi, 2016).

Abnormal default mode network (DMN), sensory network, somatomotor network (SMN), and thalamocortical network (TCN) are frequently reported in rs-fMRI studies involving DOC patients (Boly et al., 2011; Mashour and Hudetz, 2018a; Schiff et al., 2007). In

Table 1
Demographic and clinical information for the patients with disorders of consciousness (DOC).

Patient	Gender (M: male; F: female)	Months to the scan	Age (years old)	VS/MCS	Etiology	CRS-R scores Au/V/M/O/C/Ar/T
P01	M	1	21	VS/UWS	HIE	1/0/2/1/0/1/5
P02	M	2	39	VS/UWS	TBI	0/0/2/1/0/2/5
P03	M	2	16	VS/UWS	HIE	0/0/1/0/0/2/3
P04	M	2	64	VS/UWS	TBI	0/0/1/1/0/2/4
P05	M	1	62	VS/UWS	HIE	0/0/1/0/0/2/3
P06	M	2	36	VS/UWS	HIE	1/0/0/0/0/1/2
P07	M	1	43	VS/UWS	HIE	0/0/1/1/0/2/4
P08	M	1	48	VS/UWS	HIE	0/0/1/0/0/2/3
P09	M	9	32	VS/UWS	HIE	1/0/1/1/0/2/5
P10	M	1	39	VS/UWS	HIE	0/0/2/1/0/2/5
P11	M	1	62	VS/UWS	HIE	0/0/1/0/2/2/5
P12	F	1	52	VS/UWS	HIE	0/0/0/1/0/2/3
P13	M	1	30	MCS	TBI	1/1/3/2/0/2/9
P14	F	1	59	MCS	TBI	1/0/5/1/0/2/9
P15	M	3	41	MCS	TBI	1/1/3/0/0/2/7
P16	F	1	15	MCS	HIE	1/3/5/1/0/2/12
P17	F	2	20	MCS	TBI	1/1/2/1/0/2/7
P18	M	9	41	MCS	HIE	2/3/2/1/0/1/9
P19	M	3	47	MCS	HIE	1/3/0/1/0/2/7

Abbreviations: MCS, minimally conscious state; VS, vegetable state; UWS, unresponsive wakefulness syndrome; TBI, traumatic brain injury; HIE, hypoxic ischemic encephalopathy; CRS-R, Coma Recovery Scale-Revised; Au, auditory; V, visual; M, motor; O, oromotor; C, communication; Ar, arousal; T, total.

addition, abnormal functional metabolism (Fridman et al., 2014; Vanhaudenhuyse et al., 2010) and brain white matter (WM) structural connectivity (Fernandez-Espejo et al., 2012) were found in the DMN of DOC patients. Further studies also reported that the abnormal brain activity of the DMN was correlated with Coma Recovery Scale-Revised (CRS-R) scores (Rosazza et al., 2016) and could be viewed as a prognostic biomarker (Qin et al., 2015; Song et al., 2018). Moreover, abnormal FC and brain WM structural connectivity between the thalamus and the frontal cortex were reported in DOC patients (Giacino et al., 2014; Schiff, 2010; Weng et al., 2017). In sum, those studies indicated that some brain regions, such as DMN (Vanhaudenhuyse et al., 2010) and TCN (Schiff, 2010), play an important role in sustaining consciousness (Laureys, 2005; Wijdicks, 2018).

The functioning of the auditory, visual, and somatomotor regions in DOC patients is believed to be correlating with the degree of damage to consciousness. Previous studies found that the primary auditory cortex of VS/UWS patients presented similar responses to those of healthy controls when receiving stimuli using PET and fMRI (Laureys et al., 2000; Owen et al., 2005). However, compared with VS/UWS patients, minimally conscious state (MCS) patients preserved more activation areas in high level auditory processing regions (Di et al., 2007). Similar phenomena were also found in the visual and somatomotor cortices of DOC patients (Kotchoubey et al., 2013; Monti et al., 2013; Zhu et al., 2009).

Most rs-fMRI studies assumed that the temporal correlation of blood oxygen level-dependent (BOLD) signal between distinct brain regions remains steady during the scanning. In fact, this assumption may be outdated in that the pattern of brain activation changes over time (Allen et al., 2014; Chang and Glover, 2010; Vidaurre et al., 2017). Several approaches, such as sliding windows approach (Allen et al., 2014), time-frequency analysis (Chang and Glover, 2010) and hidden Markov model (HMM) (Vidaurre et al., 2017), have been applied to study the dynamic properties of brain functional configuration. Among them, the sliding windows approach has been widely used to study alterations in the brain's dynamic FC under conscious modification (Barttfeld et al., 2015; Kafashan et al., 2016; Tagliazucchi and Laufs, 2014). For example, several studies found that the brain dynamic functional properties were reduced with the decline in consciousness when subjects are asleep (Tagliazucchi and Laufs, 2014) or under anesthesia (Barttfeld et al., 2015). Altogether, these studies contributed to the comprehension of the relationship between altered consciousness and brain dynamic functional properties.

To date, few studies (Demertzi et al., 2019; Perri. et al., 2018) have examined the alteration of consciousness after severe brain injury based on dynamic framework approach. In this study, we attempted to use the sliding windows approach and hidden Markov model to understand the properties of dynamic functional connectivity (dFC) associated with consciousness in DOC patients. Previous rs-fMRI studies (Giacino et al., 2014; Mashour and Hudetz, 2018b; Schiff, 2008) reported abnormal FC patterns of several cortical and subcortical regions in DOC patients but lacked detailed spatial-temporal information to interpret these abnormal brain network alterations. In the calculations, we first applied an independent component analysis (ICA) to select the intrinsic components (ICs) within the whole-brain, then used a sliding windows approach to construct dFC matrices for each subject. We applied the *k*-means clustering algorithm to cluster these matrices. To overcome a drawback of the sliding windows approach, we also used a hidden Markov model (HMM) to test the robustness of the result. Finally, we applied connectome-based predictive modeling (CPM) to assess the clinical predictability of CRS-R in the patients and used support vector machine (SVM) to predict patients' diagnostic status.

2. Materials and methods

2.1. Participants

A total of 45 DOC patients were recruited from the Liuhuaqiao Hospital in Guangzhou, China. Each patient was assessed using the CRS-R (Kalmar and Giacino, 2005), which consists of a total of 23 items and 6 subscales that test auditory, visual, motor, oromotor, communication, and arousal functions. The exclusion criteria for the patients were as follows: (1) history of alcohol or drug abuse, (2) previous psychiatric or neurological illness, and (3) extensive focal brain damage. Fig. 1 shows the patients who were excluded for the above reasons and those who exhibited excessive head-motion. In the end, we retained the data from 19 DOC patients (14 M/ 5 F; aged 39.0 ± 14.6 years old) after excluding 26 patients' fMRI data for the above reasons. Based on this behavioral assessment, 12 patients were diagnosed as VS/UWS and 7 patients as MCS. The detailed demographic and clinical information for the DOC patients is listed in Table 1 and exhaustive etiological information about DOC patients could be found in Table S1. We also recruited 19 healthy volunteers (11 M/ 8 F; aged 32.2 ± 6.9

years old) as a control group. This study was approved by the Ethics Committee of the Liuhuaqiao Hospital. Written informed consent in the study was obtained from the legal representatives of the DOC patients and from the healthy controls.

2.2. Image acquisition

All MRI data were acquired on a GE 3T MR scanner with an eight-channel phased-array head coil. The rs-fMRI data were obtained using a single-shot multi-slice gradient-echo echo-planar imaging (GE-EPI) sequence. The sequence parameters were as follows: repetition time (TR) = 2000 ms, echo time (TE) = 26 ms, flip angle (FA) = 90°, field of view (FOV) = 240 × 240 mm^2, data matrix = 64 × 64, slice thickness = 3.6 mm, inter-slice gap = 0.6 mm, 36 axial sequential slices, and 240 volumes acquired in about 8 min. High-resolution brain structural images were also acquired using a T1-weighted 3D fast spoiled gradient recalled (FSPGR) sequence with the following parameters: TR = 8.86 ms, TE = 3.52 ms, FOV = 240 × 240 mm^2, data matrix = 256 × 256, FA = 90°, voxel size = 0.94 × 0.94 × 1 mm^3, and 176 sagittal slices covering the whole-brain.

2.3. Data preprocessing

Fig. 2 illustrates the flowchart of the data analysis steps. First, we preprocessed the raw rs-fMRI data and used ICA to select the independent components (ICs). Then, we calculated the FC matrices of those ICs in each window (window length = 22 TRs, step = 1 TR) and used the *k*-means clustering algorithm to cluster these matrices. Next, we chose HMM to describe the time series of functional signal in different brain region by using discrete number of states, and then to test the robustness and replicability of the results obtained from the sliding windows approach. Finally, we applied CPM to predict the CRS-R scores of the DOC patients.

The rs-fMRI data were preprocessed using SPM12 (http://www.fil.ion.ucl.ac.uk/spm). We removed the first 10 image volumes, performed slice-timing, and corrected the head-motion. In this study, the fMRI data were used only if the head motion satisfied a translation of less than 3 mm in any direction and a rotation of less than 3° in any axis. Subsequently, the functional images were co-registered to high-resolution T1-weighted brain structural images, which were segmented into GM, WM, and CSF; then we registered the segmented GM images to MNI space. The normalized functional images were resampled to a voxel size of 3 mm^3 and smoothed with a 5 mm full width at half-maximum (FWHM) Gaussian kernel.

2.4. Group ICA and postprocessing

We used GIFT (4.0b, http://mialab.mrn.org/software/gift) (Calhoun et al., 2001) to decompose the preprocessed rs-fMRI data into spatially independent and temporally coherent components. Before running the group ICA, we *z*-scored the time series in each voxel to normalize the spatial variance. Then, we selected a high model order to obtain cortical and subcortical functional parcellations. We retained 120 principal components (ICs) using principle component analysis (PCA) and then used an expectation maximization (EM) algorithm to decompose all the subjects' reduced data into 100 ICs. For the estimation stability, we ran the Infomax group ICA in ICASSO 20 times. A group ICA (GICA) back-reconstruction was used to estimate the subject-specific spatial maps and time series. We selected the 43 ICs whose peak activations were located in the GM rather than the WM or ventricles as intrinsic connectivity networks (ICNs). The following steps were performed on the time courses of the 43 ICs to reduce the remaining noisy signals: (1) linear, quadratic, and cubic detrending, (2) multiple regression of the 6 head motion parameters and their temporal

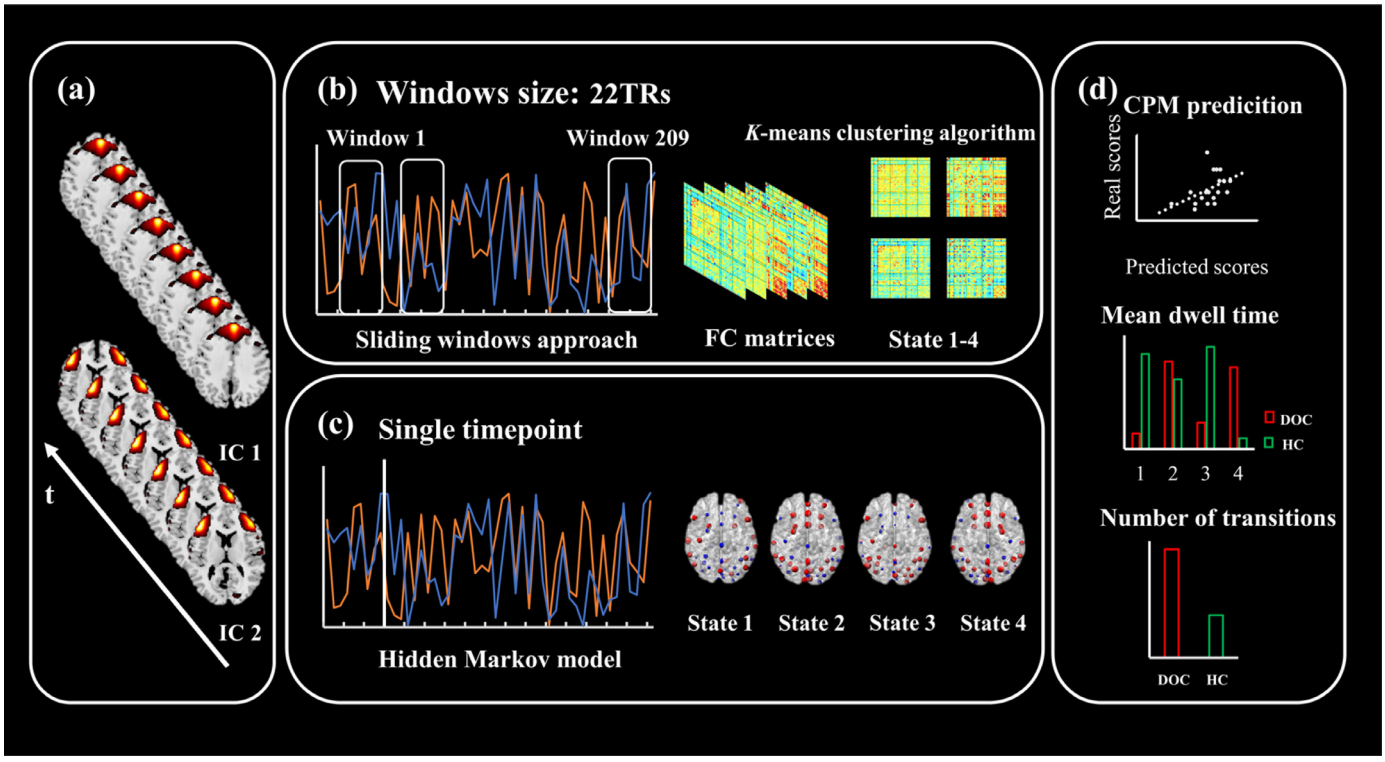

Fig. 2. Flowchart for analyzing the properties of the dynamic functional connectivity (dFC) states in patients with disorders of consciousness (DOC) and healthy controls (HC). a) A total of 43 intrinsic components (ICs) were selected using independent component analysis (ICA). b) The dFC was estimated by calculating the inter-ICs temporal correlation within a siding window. Then four states were clustered by the *k*-means clustering algorithm. c) The robustness of the results was tested by the hidden Markov model (HMM). d) Connectome-based predictive modeling (CPM) was used to predict the CRS-R scores. We used a two-sample *t*-test to examine the between-group differences in the temporal properties of the dFC and the HMM.

derivatives, (3) low pass filtering by removing high frequencies beyond 0.15 Hz, and (4) exclusion of detected outliers.

2.5. Dynamic functional connectivity (dFC) networks and clustering

To obtain each subject's dFC matrices, we calculated the Pearson correlation between each pair of ICs timeseries by using tapered sliding windows. We selected 22 TRs (44 s) as window lengths and a Gaussian (σ = 3 TRs) to convolve a tapered window, resulting in 209 windows by sliding in steps of a single TR every time. An L1 (Manhattan distance) penalty was imposed on the precision matrix (inverse of the correlation matrix) to raise its sparsity. The windows size was established at 22 TRs (44 s) because 30 s to 60 s has been deemed reasonable and was used in previous studies (Allen et al., 2014; Damaraju et al., 2014). This range reaches a satisfactory temporal trade-off between the real dynamic fluctuation and the reliable temporal information (Preti et al., 2017).

To assess the re-occurrence of the dFC patterns, we used the *k*-means clustering algorithm to cluster those FC matrices that were obtained from all the subjects in the present study. The correlation distance function was chosen as a *k*-means clustering algorithm because this approach has the advantage of reflecting the FC pattern regardless of magnitude (Damaraju et al., 2014). Then $k = 4$ was determined as the number of clusters by using the elbow-criterion (a ratio of within-cluster distance to between-cluster distance), and the result was similar to the *k* values for 3 and 5.

2.6. Statistical analysis

These group differences in dFC were determined using a two-sample *t*-test and corrected by a false discovery rate correction (FDR, $q < 0.05$). In addition, we calculated the mean dwell time (*MDT*) and the number of transitions (*NT*) to examine the group differences in the temporal properties. The *MDT* was calculated as the mean number of successive windows assigned in one state, and *NT* was the number of times one state transited to another.

2.7. Hidden Markov model (HMM)

To test the robustness of the results obtained from the sliding windows approach, we re-processed the data using the hidden Markov model-multivariate autoregressive toolbox (Vidaurre et al., 2018, 2017). The HMM had the basic assumption that the fMRI time series data could be depicted and represented by a series of discrete brain states that recur with time. The number of discrete brain states was selected as 4 because that was the number of states identified by the sliding windows approach.

The functional data were preprocessed in accordance with the previous preprocessing steps used in the sliding windows approach. These ICs were set as ROIs to extract the time series (mean was zero and standard deviation was units). After temporally concatenating all the subjects' time series data, we applied the HMM to estimate the brain states at the group level. We ran the random initialization algorithm 5 times to acquire a stable estimate. Then the variational inference algorithm was repeated 10 times to ensure that the procedure could skip the local minima and find the global best solution. Then we calculated each subject's specific brain state to obtain the *MDT* and the transition rate counted as the number of transitions (*NT*) per second that correspond to the similar parameters used in the sliding windows approach. A two-sample *t*-test was used to test the significant difference in the *MDT* and the transition rate between the DOC patients and the healthy controls.

2.8. Connectome-based predictive modeling and support vector machine

We applied the CPM method (Shen et al., 2017) to assess the prediction ability of dFC for the CRS-R scores of the DOC patients. Specifically, this method has four steps: (1) choosing features, (2) summarizing features, (3) constructing and applying the model, and (4) evaluating the significance of the prediction. First, to acquire representative information from the dFC, we extracted the mean dFC by averaging the FC in all the windows for every DOC patient. Next, we used a leave-one-out cross-validation (LOOCV) by splitting patients into a training set (subjects = 18) and a testing set (subject = 1) to assess the generalization performance of the predicted result. In the training set, to reduce the influence of outliers and obtain a stable result, we calculated the robust regression correlation between every edge represented in the mean dFC and the CRS-R scores. A threshold ($p < .05$) was applied to select the edges that were significantly correlated with the clinical scores. The strength values (correlation value) of those significant relevant edges were added together for each subject. Then, we used the sum value and the clinical scores to build a linear model to predict the clinical scores of the subject in the testing set. Finally, we computed the correlation between the predicted clinical scores and the real CRS-R scores to obtain the predictive performance.

To validate the significance of the *r*-values generated from the clinical scores and the predicted scores from the LOOCV, we iterated 1000 permutations. To generate a new predicted score, we assigned the shuffled clinical scores to the subject before running the LOOCV. Finally, we calculated the *p*-value by dividing the position of the true prediction *r*-value in the random prediction *r*-value by the number of permutations.

By taking *NT* and *MDT* of the four states as features, we applied a linear support vector machine (SVM) classifier to discriminate MCS patients from VS/UWS patients. The patients were split up into a training set (18 subjects) and a testing set (1 subject). We used the leave-one-out cross-validation (LOOCV) to evaluate the performance of the classifier. We first trained the SVM classifier based on features of the training set and then used this classifier to predict a single-subject' diagnosis status in the testing set. With the LOOCV, we estimated the accuracy of the classifier by using the rate of correctly predictive number and the number of all subjects. After the true classifier accuracy being obtained, we randomly assign the data labels to different subjects and recomputed the classifier accuracy. These steps were iterated 1000 permutations to generate an empirical null distribution of the classifier accuracy. Finally, the threshold of significance of classifier accuracy was set at $p < .05$ based on the distribution result of permutation test.

In addition, we used Spearman's rank correlation coefficient to assess the relationships between these indices (*NT* and *MDT* for the four states) and CRS-R scores in the patient group and set the threshold for significant level at $p < .05$.

3. Results

3.1. Demographic and clinical information

The demographics and the statistical clinical information are listed in Table 2. No differences in age or gender were found between the two groups.

3.2. Intrinsic connectivity networks

Fig. 3 shows the spatial maps of the obtained 43 intrinsic ICs. The labels and peak coordinates for all these ICs are provided in Table S2 (Supplementary Materials). Considering their anatomical locations and functional properties, we classified these ICs into seven sub-networks, the auditory (AUN), somatomotor (SMN), cerebellar (CBN), cognitive control (CCN), default mode (DMN), visual (VSN), and subcortical networks (SCN). In fact, the classification of ICs was similar to that of previous studies (Allen et al., 2014; Rashid et al., 2014).

The AUN comprised two symmetrical ICs whose activations were located in the bilateral superior temporal gyrus (STG). The region of the CBN included three ICs, which included most of the cerebellum. The

Table 2
Demographic and clinical statistical information for the patients with disorders of consciousness (DOC) and the healthy controls (HC).

Characteristics	DOC	HC	Statistics	*p*-value
Age (years old)	39.0 ± 14.6	32.2 ± 6.9	$t = 1.83$	0.08[a]
Gender (male/female)	15/4	11/8	$\chi^2 = 1.94$	0.16[b]
Months to the scan	2.73 ± 2.79			
Etiology (HIE/TBI)	12/7			
Diagnosis (UWS/MCS)	12/7			

Abbreviations: HIE, hypoxic ischemic encephalopathy; TBI, traumatic brain injury; MCS, minimally conscious state; UWS, unresponsive wakefulness syndrome.
[a] Two-sample *t*-test.
[b] χ^2 test.

CCN included 9 ICs. The DMN consisted of 11 ICs. The SCN contained only 1 IC, which was activated in the bilateral putamen. The SMN consisted of 8 ICs. The VSN included 9 ICs, which were centered in the occipital cortex.

3.3. Group differences in dynamic functional connectivity (dFC)

After acquiring 209 FC matrices for each subject, we using a *k*-means clustering algorithm to divide all the windows into 4 states (Fig. 4), which were represented by their centroids (cluster medians). State 1, occupying the majority of the windows, showed sparse and weak dFC in the SMN, CCN, and DMN. State 2 exhibited positive intra- and inter-connectivity in the CCN, VSN, SMN, and DMN. In addition, the VSN correlated positively with the DMN and CCN. State 3 displayed strong and dense inter- and intra-network dFC in the VSN and SMN. State 4 showed positive intra- and inter-network dFC in the VSN and DMN.

Fig. 5 shows the centroids of the states for the DOC patients and for the controls. Because the *MDT* in State 2 of the healthy controls was less than one, we added it in Fig. S1 (Supplementary Materials). The *MDT*s for each group are shown in Fig. 6a. In brief, we found that the DOC patients had a significantly shorter *MDT* in State 1 ($t = -4.65$, $p < .001$) and a longer *MDT* in State 2 ($t = 4.33$, $p < .001$) than the healthy controls. We also found State 4 was only detected in the DOC patients. In addition, we calculated the between-group difference in *NT* and found that the DOC patients changed more often ($t = 2.36$, $p = .024$) than the healthy controls (Fig. 6b). Fig. 6c summarizes the group-differences in dFC between the ICs pairs. For each dFC state, we calculated group difference in FC between the DOC patients and healthy controls. We found that in State 3 instead of other states, the patients showed significantly lower intra- and inter-network dFC in the VSN, SMN, and AUN than the healthy controls.

3.4. Hidden Markov model (HMM)

Fig. 7 shows the 4 states and the between-group difference in temporal properties of those states obtained using HMM. We found

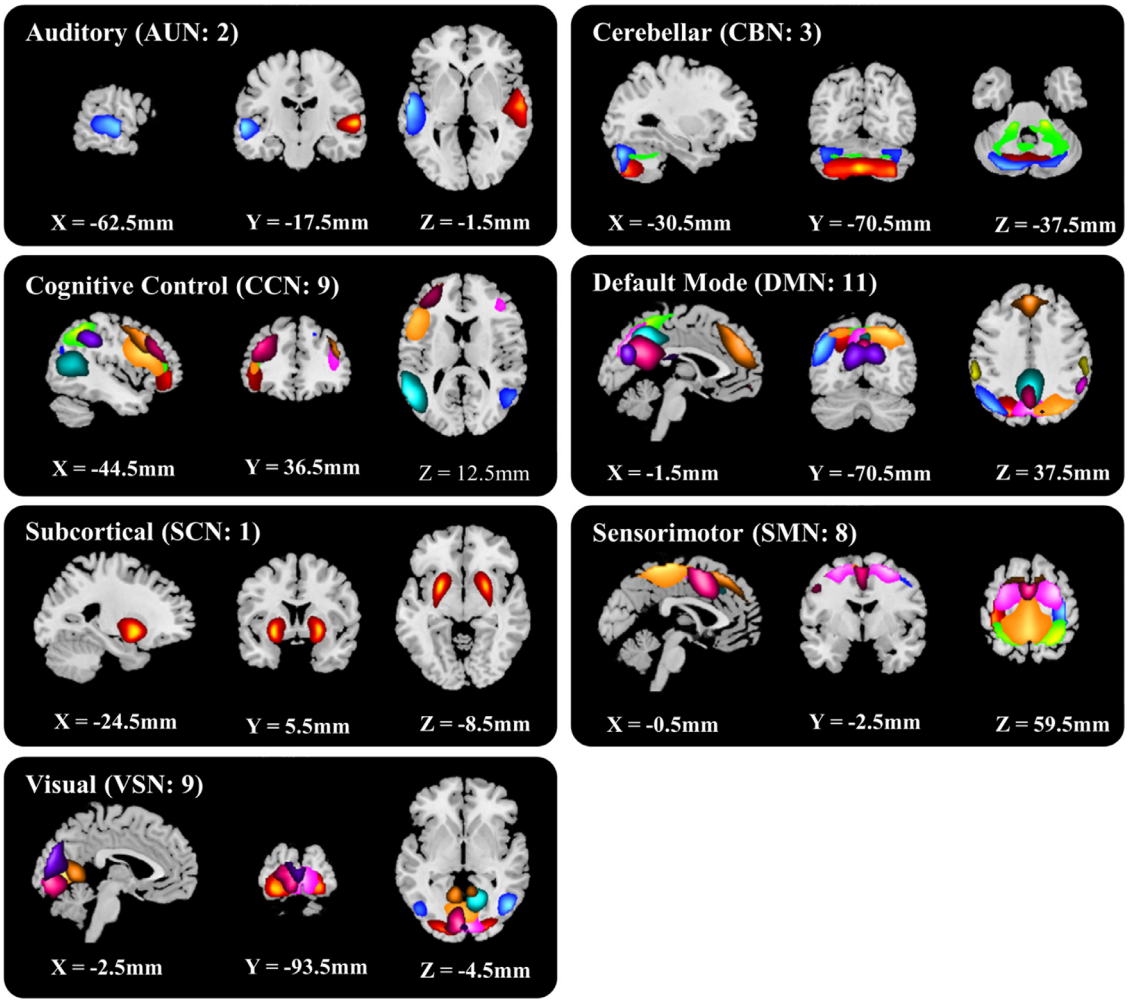

Fig. 3. Spatial maps of the 43 selected independent components (ICs) for patients with disorders of consciousness (DOC) and healthy controls (HC). Based on their anatomical and functional properties, we classified these ICs into seven sub-networks. Different colors indicate the identified ICs in the spatial maps.

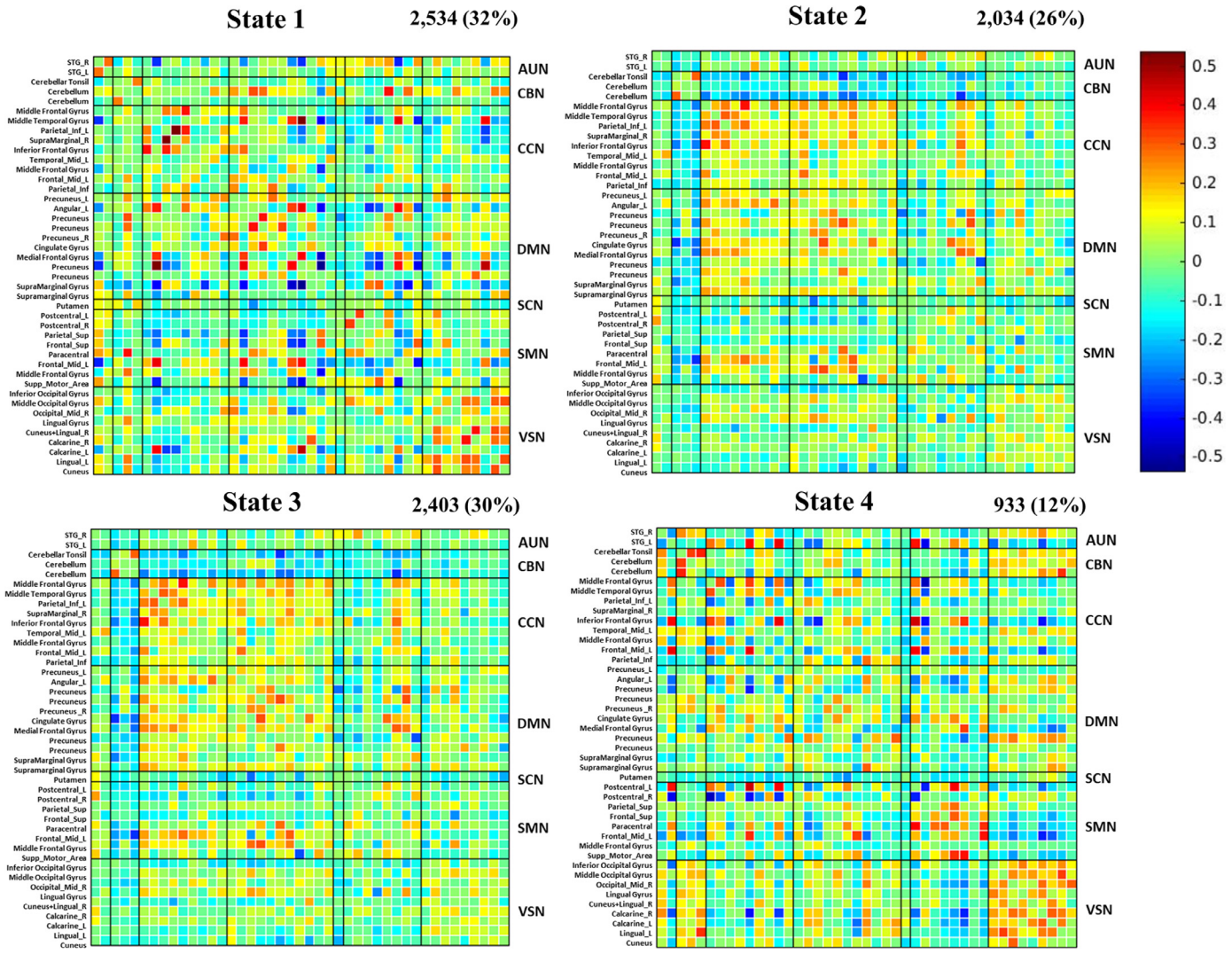

Fig. 4. The four dFC states for patients with disorders of consciousness (DOC) and healthy controls (HC). The total number and the percent of temporal occurrences are listed above each centroid.

that, compared with the healthy controls, the DOC patients had a significantly longer *MDT* in States 2 and 4 but shorter *MDT* in States 1 and 3 (State 1: $p < .001$; State 2: $p = .006$; State 3: $p < .001$; State 4: $p < .001$, Fig. 7b). The DOC patients showed (transition rate = 0.031) significantly more switching behavior than the controls (transition rate = 0.008, $t = 3.618$, $p < .001$).

3.5. Connectome-based predictive modeling and support vector machine

Pearson's correlation coefficient ($r = 0.446$) between the predicted and observed scores was estimated using the LOOCV. With the non-parametric permutation *t*-test, we showed that the CPM could significantly ($p = .015$) predict the CRS-R scores of a new subject (Fig. 7d). Although we put all of the positive and negative dFC into the prediction model, we found that the negative dFC, but not the positive dFC, was significantly correlated with the CRS-R scores.

We found the *NT* had ability to discriminate the MCS patients from the VS/UWS patients. When taking the *NT* as features to predict patients' diagnostic status, we found that the classification accuracy could reach up to 73.68% ($p = .001$, sensitivity to 75.00%, and specificity to 71.43%) (Fig. 8a). However, when taking the linear SVM classifier and selecting *MDT* as features to discriminate the MSC patients from VS/UWS patients, we found a chance level accuracy. In addition, using Spearman's rank correlation, we found a significant positive correlation ($r = 0.540$, $p = .017$) between *NT* and the CRS-R scores in DOC patients (Fig. 8b). However, no significant correlation was found between *MDT* in any state and the CRS-R scores (State 1: $r = 0.075$, $p = .418$; State 2: $r = 0.418$, $p = .197$; State 3: $r = 0.308$, $p = .247$; State 4: $r = 0.107$, $p = .381$).

4. Discussion

In this study, we used a sliding windows approach to analyze the dynamic functional properties of the DOC patients. We found that the DOC patients displayed reduced dFC within the visual, auditory, and somatomotor networks and had a greater number of transitions (*NT*) than the healthy controls. The robustness of the result was tested using HMM. From the CPM analysis, we found that the dFC could be used to predict a patient's clinical scores. Those results extended our knowledge of the altered dFC in the DOC patients.

4.1. Group differences in state

A total of 4 states were identified in either or both of the DOC patients and controls using the *k*-means clustering algorithm (Fig. 4). This means the FC fluctuated over time rather staying at stationary in the DOC patients. The number of clusters was similar to that reported in a previous study, in which Demertzi et al. (2019) analyzed brain

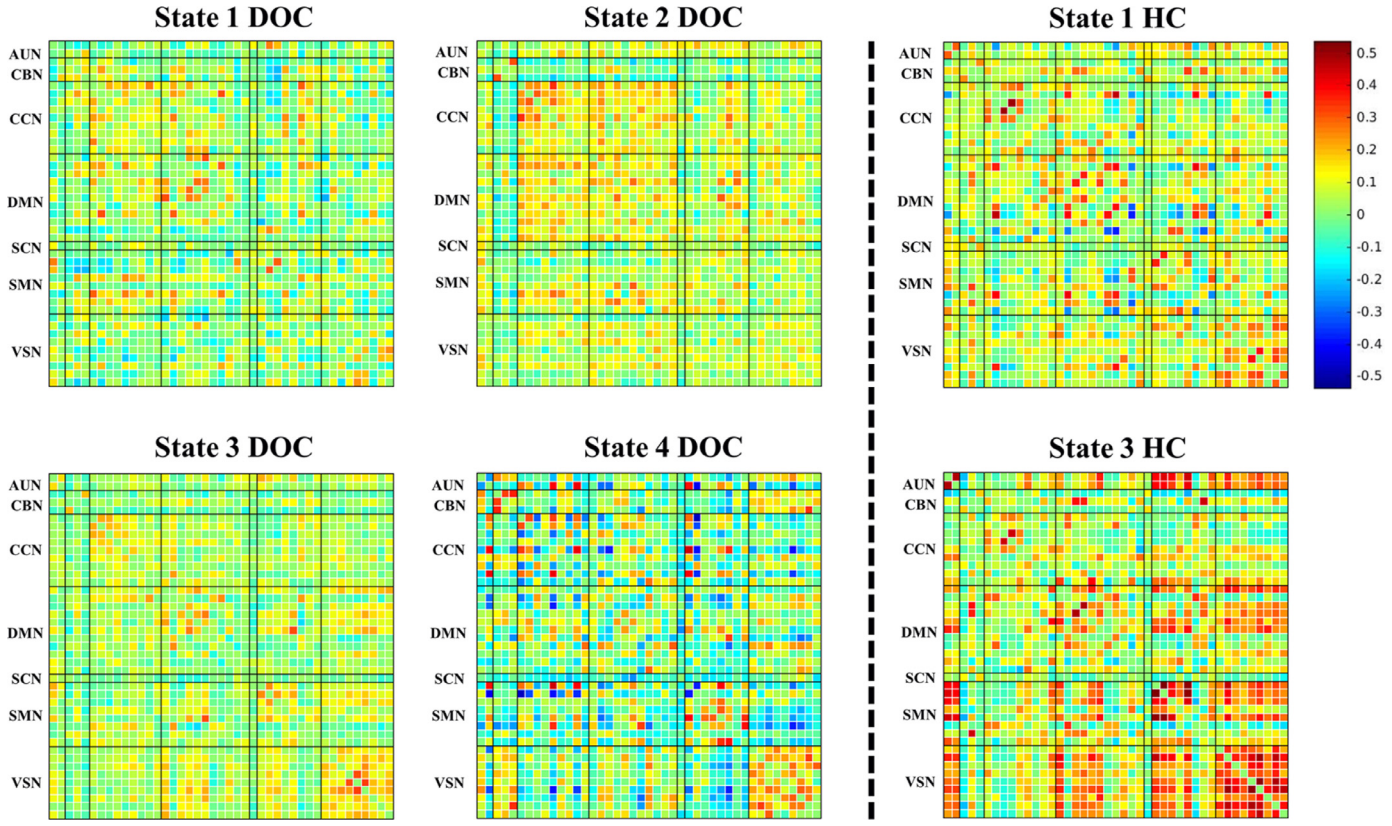

Fig. 5. Detailed group centroids of the dFC states for patients with disorders of consciousness (DOC) and healthy controls (HC).

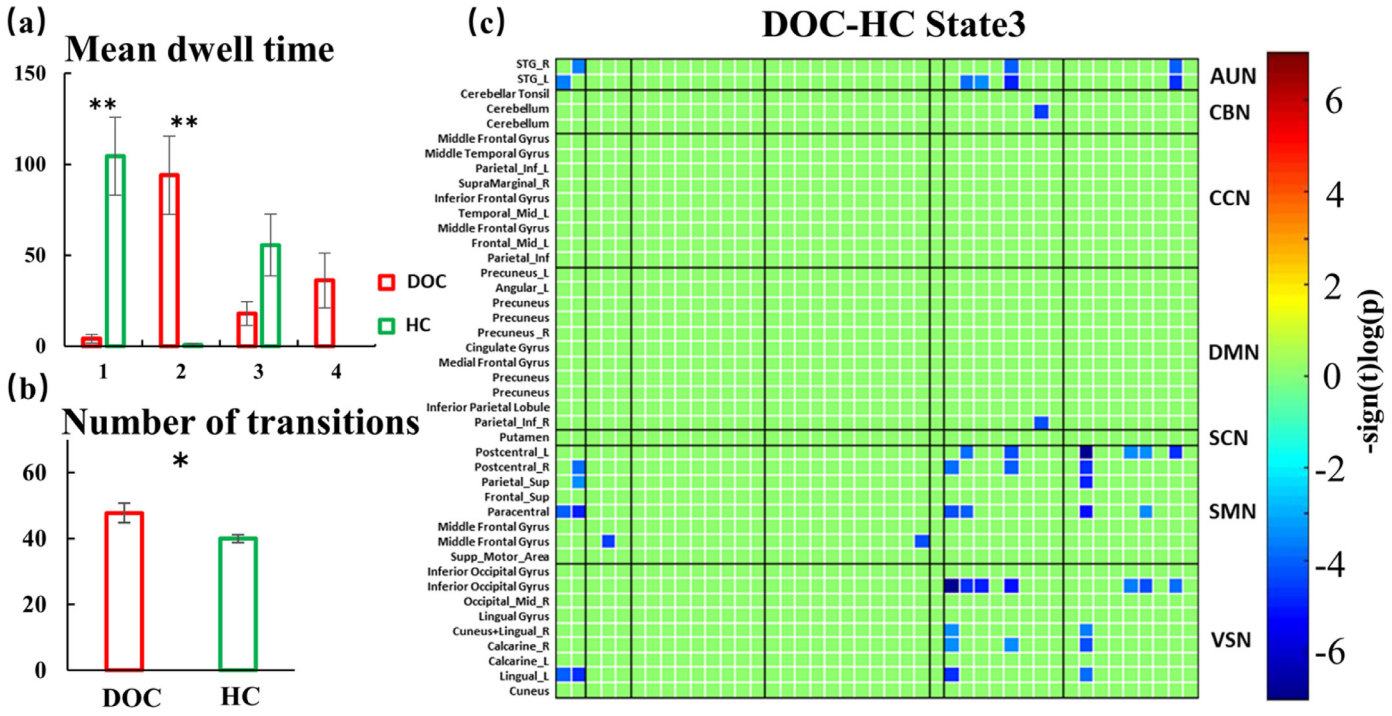

Fig. 6. Between-group differences in temporal properties of the dFC states derived using the sliding windows approach. (a) The mean dwell time (*MDT*). (b) The number of transitions (*NT*) for each group. (c) The group differences in dynamic functional connectivity (dFC) in State 3 (two-sample *t*-test, FDR correction, $q < 0.05$). Notes: * indicates $p < .05$; ** indicates $p < .001$. We did not calculate the *p* value of the *MDT* in State 4 because this state was not found in the healthy controls.

dynamics of DOC patients by using a dynamic functional coordination approach, detected 4 patterns of functional signal coordination associated with conscious and unconscious states. Based on the distribution of *MDT* between the patient and control groups (Fig. 6a), we divided the four states in two types, common states, which were found in both the DOC patients and the heathy controls, and altered states, which were mainly found in the patients. This phenomenon is also found in previous studies (Li et al., 2014; Ou et al., 2014). For example,

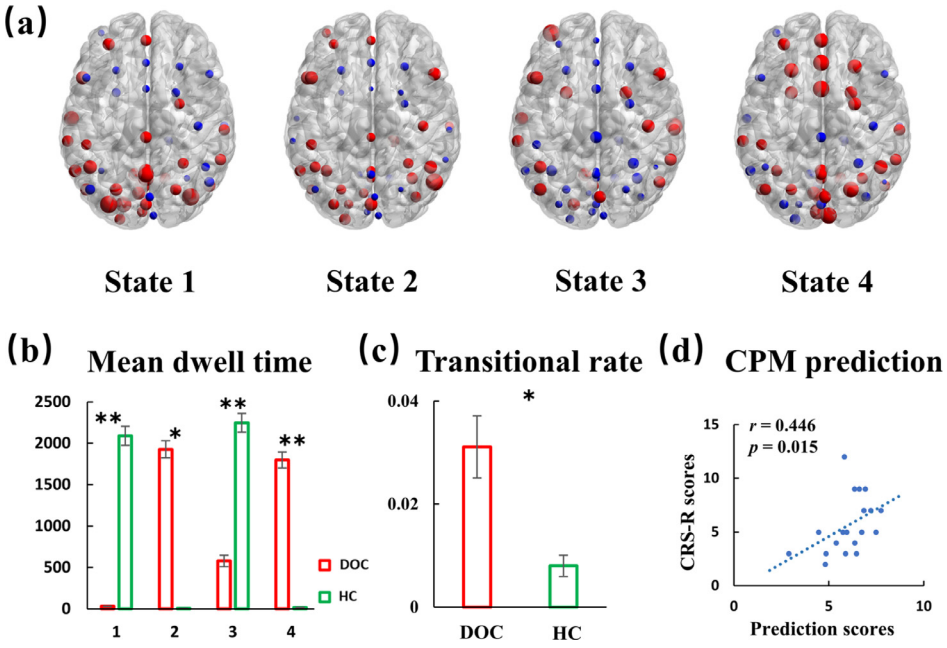

Fig. 7. The four states and between-group differences in their temporal properties derived from the hidden Markov model (HMM) for patients with disorders of consciousness (DOC) and healthy controls (HC). (a) The four states of all the subjects. The nodes color-coded in red (blue) represent the nodes with a positive (negative) activation in the given state. (b) The mean dwell time for each state. (c) The transitional rate for each group. (d) Connectome-based predictive modeling (CPM) predicted the CRS-R scores of every subject. Notes: *, $p < .05$; **, $p < .001$. (For interpretation of the references to color in this figure legend, the reader is referred to the web version of this article.)

Li et al. (2014) reported that two altered states in post-traumatic stress disorder (PTSD) patients could act as biomarkers for distinguishing patients from controls. Specifically, the two altered states (Fig. 5), States 2 and 4, displayed relatively weak dFC inter- and intra- AUN, VSN, and SMN compared with the common states. This result was consistent with previous studies (Demertzi et al., 2015; Vanhaudenhuyse et al., 2010) and suggests that some of the dynamic functional interactions had been inactivated.

4.2. Group differences in dynamic functional connectivity (dFC)

We found that the significant between-group differences in dFC (Fig. 5c) were mainly associated with the AUN, VSN, and SMN. This result was similar to a previous study (Demertzi et al., 2019) which adopted a dynamic functional coordination analysis and found widely decreased FC (not only in intra- and inter-network FC but also long-distance FC) in the whole brain of DOC patients compared with health controls. In the AUN, the DOC patients showed decreased dFC between the right STG and left STG compared with the healthy controls. This result is in line with previous studies of DOC patients (Demertzi et al., 2015, 2014). The STG is believed to process sound information (Friederici et al., 2017) and comprehend language (Wise et al., 2001). Demertzi et al. (2014) analyzed the FC of different networks of DOC patients and found that the auditory network, including the STG, was one of the most severely damaged regions compared with healthy controls. Subsequently, a study (Demertzi et al., 2015) found the FC of this region could be used to distinguish MCS patients from VS/UWS patients. Overall, there seems to be some evidence to indicate that the STG is associated with the abnormal auditory response in DOC patients.

In this study, we found that the DOC patients showed decreased dFC between the right postcentral gyrus and the left postcentral gyrus, between the paracentral gyrus and the right postcentral gyrus, and between the paracentral gyrus and the left postcentral gyrus in the SMN (Fig. 6c) compared with the controls. This result is consistent with several previous studies (Kotchoubey et al., 2013; Ovadia-Caro et al., 2012; Yao et al., 2015). In addition to decreased FC (Ovadia-Caro et al., 2012), Yao et al. (2015) found a positive correlation between the amplitude of low-frequency fluctuation (ALFF) in the postcentral gyrus and the fractional anisotropy of the posterior thalamic radiation in DOC patients. Kotchoubey et al. (2013) found the weighted global connectivity of the postcentral gyrus could help in differentiating between VS/UWS patients or MCS patients. Moreover, Perri et al. (2016) reported that the FC between the paracentral gyrus and the DMN was positively correlated with the conscious state (from VS/UWS patients, MCS patients, to controls). Altogether, our study showed that the postcentral and paracentral gyrus seem to be associated with the

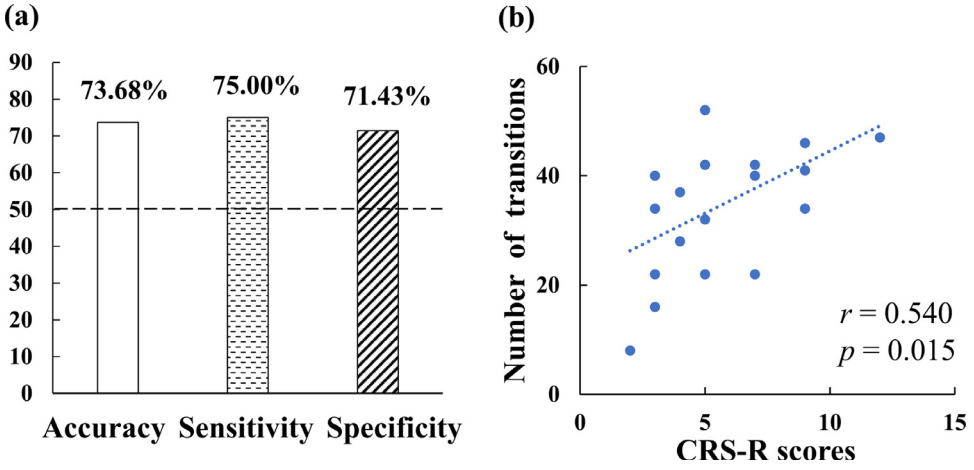

Fig. 8. Performance of support vector machine (SVM) to predict the diagnostic status and the correlation between the number of transitions (*NT*) and clinical scores for DOC patients. (a) Bar plot of different predictive performance. Using the *NT* as a feature, we estimated the classification accuracy (73.68%), sensitivity (75%), and specificity (71.43%) for predicting patients' diagnostic status. The dashed line represents the chance level (50%). (b) Scatter plot of the correlation between the number of transitions and the CRS-R scores. The dotted line corresponds to the best fit ($r = 0.54$, $p = .015$).

impaired somatosensory function in DOC patients.

Several significantly decreased between-group dFCs were found in the VSN. Compared with the controls, reduced dFC was found between the inferior occipital gyrus and the cuneus/the right lingual gyrus, between the inferior occipital gyrus and the right calcarine gyrus, and between the inferior occipital gyrus and the left lingual gyrus in the DOC patients (Fig. 6c). Monti et al. (2013) reported that DOC patients still preserved some visual cognitive function when receiving visual stimuli. The current study also showed group differences in inter-network dFC between the AUN, SMN, and VSN. This result is compatible with previous studies (Amico et al., 2017; Demertzi et al., 2015). Demertzi et al. (2015) found that the inter-network FC between the auditory and visual networks could be used to classify patients into the correct categories (MCS or VS/UWS patient). Amico et al. (2017) reported abnormal inter-network FC between the VSN and SMN by extracting ICA traits in DOC patients. Taken together, our finding of abnormal dFC in the DOC patients may be associated with the dysfunction of sensory and somatomotor processing.

4.3. Dynamic functional connectivity (dFC) predict CRS-R scores

The decreased dFC was mainly located in the SMN, AUN, and VSN, and the functions of those networks were related to the measured items of the CRS-R. Using CPM, we found that the dFC could be used to predict the scores of the DOC patients ($r = 0.446$, $p = .015$). In addition, we noticed that the negative edges, rather than the positive edges, could be used to predict the CRS-R scores. Using a dynamic causal model, Chen et al. (2018) found that only negative effective connectivity could predict CRS-R scores in DOC patients**.** Our findings indicated that the dFC might be useful for diagnosing a patient's state of impairment.

4.4. Group difference in number of transitions (NT)

The between-group difference in *NT* could be understood from the organization of the brain network. Modularity provides a measure for evaluating the segregation and integration of networks (Bullmore and Sporns, 2009; van den Heuvel and Sporns, 2019). High modularity indicates that the nodes densely connect with each other within a network but sparsely connect between networks. Although integration can enhance the brain's working efficiency (van den Heuvel and Sporns, 2019), maintaining segregation is also advantageous for supporting cognitive ability (Gallen et al., 2016; Grady et al., 2016), resistance to damage (Nomura et al., 2010; Siegel et al., 2016), and meeting task processing demands (Bassett et al., 2015; Cohen and D'Esposito, 2016). Godwin et al. (2015) found that brain modularity may be basic for generating awareness. Taking these findings together, the network organization in healthy controls appears to reach an optimal state between integration and segregation (Raichle, 2015).

It is possible that our results refect the effect of severe brain damage, which caused an unstable brain situation in brains (Alexander-Bloch et al., 2010). Previous several studies (Crone et al., 2014; Demertzi et al., 2019) showed that DOC patients had lower modularity than healthy controls. However, no significant difference was found in either path length or the global efficiency between DOC patients and healthy controls (Crone et al., 2014). In addition, a diffusion tensor imaging (DTI) study (Weng et al., 2017) also found that DOC patients showed a reduced clustering coefficient and lower local efficiency, which implies that the balance between segregation and integration was broken. These studies indicated that the patients may possibly enter a disturbed situation in which they retain the ability to integrate but lose the ability to segregate. Using SVM approach, we found that the *NT* could be used as a potential biomarker for predicting patient's diagnostic status (VS/UWS and MCS). We also found that the *NT* was positively correlated with CRS-R scores in the patients. Therefore, our *NT* results may indicate that DOC patients were in an unstable state and this index may reflect altered consciousness after sever brain injury.

4.5. Relationship between dFC and brain activation

After using the sliding windows approach to determine the number of states, the distribution of the *MDT*, and the *NT* for two groups, we found that these temporal properties were similar to the results from the HMM. Specifically, the DOC patients showed a greater number of states and number of transitions (*NT*) than the healthy controls. From a methodological perspective, although the two approaches that we used are data-driven methods to cluster the states, the sliding windows approach produced the dynamic patterns of the FC between brain regions and the HMM gave the patterns of activity across the subjects' brain regions. This study, which combined FC with brain activation, may provide new insights for exploring brain properties. Recent studies found there was an association between BOLD activity and FC (Fu et al., 2018; Tomasi and Volkow, 2018). Fu et al. (2018) reported that aberrant coupling between dynamic ALFFs and dFC measures occurs in schizophrenia. Tomasi and Volkow (2018) found that the local FC density (lFCD) showed a linear relationship with ALFF and that the lFCD could be used to predict the BOLD activation patterns. Taken together, our findings suggest that FC and brain activation have the same physiological foundation.

4.6. Limitations

This study has several limitations. First, although a total of 45 DOC patients were recruited at the time we did the scanning, we were only able to utilize 19 patients for the analysis. There was an agonizing trade-off between subject quantity and image quality. The extensive brain lesion in some patients would have produced poor normalization results and overlarge head-motions would have introduced artifacts. The results of the specific exclusion process are shown in Fig. 1. Second, although the sliding windows approach has been widely used to study the dynamic properties of the brain, this method has an unsolved issue in that the length of the windows is decided by rule of thumb, not by a gold standard (Preti et al., 2017). However, HMM does not need to overlap in time when it is used to calculate dynamic properties. This is the reason that we chose the HMM as a supplemental approach to test the robustness of our result. Third, previous studies found that the thalamus was involved in the abnormal functioning of the corticothalamic system in DOC patients (Fridman et al., 2014; Schiff, 2010). However, we did not find such a result for the thalamus in the subcortical region using a high order ICA model. This result may be associated with serious thalamic impairment in DOC patients (Adams et al., 2000).

In summary, we analyzed the dFC across the whole-brain in DOC patients using a sliding windows approach and a hidden Markov model. We found that, compared with the healthy controls, the patients had a greater number of states and number of transitions (*NT*) among the states as well as displaying a reduced dFC in the auditory, visual, and somatomotor networks. Using CPM, we found that the dFC could be used to predict the CRS-R scores of the DOC patients and, using SVM, the *NT* was capable to be used to discriminate VS/UWS patients from MCS patients. These findings may provide a deeper insight into the pathophysiology mechanisms of this disease.

Declaration of Competing Interest

The authors declare that they have no competing financial interests.

Acknowledgments

The study was supported by grants from the National Natural Science Foundation of China (Grant numbers: 81871338, 81371535, and 81271548) and the National Key R&D Program of China (Grant

number: 2018YFC1705006). The funding organizations played no further role in the study design, data collection, analysis and interpretation, or paper writing. We appreciate the content and English editing assistance of Drs. Rhoda E. and Edmund F. Perozzi.

Supplementary materials

Supplementary material associated with this article can be found, in the online version, at doi:10.1016/j.nicl.2019.102071.

References

Adams, J.H., Graham, D.I., Jennett, B., 2000. The neuropathology of the vegetative state after an acute brain insult. Brain 123 (Pt 7), 1327–1338.

Alexander-Bloch, A.F., Gogtay, N., Meunier, D., Birn, R., Clasen, L., et al., 2010. Disrupted modularity and local connectivity of brain functional networks in childhood-onset schizophrenia. Front. Syst. Neurosci. 4, 147. https://doi.org/10.3389/fnsys.2010.00147.

Allen, E.A., Damaraju, E., Plis, S.M., Erhardt, E.B., Eichele, T., et al., 2014. Tracking whole-brain connectivity dynamics in the resting state. Cereb. Cortex 24 (3), 663–676. https://doi.org/10.1093/cercor/bhs352.

Amico, E., Marinazzo, D., Di Perri, C., Heine, L., Annen, J., et al., 2017. Mapping the functional connectome traits of levels of consciousness. Neuroimage 148, 201–211. https://doi.org/10.1016/j.neuroimage.2017.01.020.

Barttfeld, P., Uhrig, L., Sitt, J.D., Sigman, M., Jarraya, B., et al., 2015. Signature of consciousness in the dynamics of resting-state brain activity. Proc. Natl. Acad. Sci. USA 112 (3), 887–892. https://doi.org/10.1073/pnas.1418031112.

Bassett, D.S., Yang, M.Z., Wymbs, N.F., Grafton, S.T., 2015. Learning-induced autonomy of sensorimotor systems. Nat. Neurosci. 18 (5). https://doi.org/10.1038/nn.3993.744–+.

Boly, M., Garrido, M.I., Gosseries, O., Bruno, M.A., Boveroux, P., et al., 2011. Preserved feedforward but impaired top-down processes in the vegetative state. Science 332 (6031), 858–862. https://doi.org/10.1126/science.1202043.

Bosco, A., Lancioni, G.E., Belardinelli, M.O., Singh, N.N., O'Reilly, M.F., et al., 2010. Vegetative state: efforts to curb misdiagnosis. Cognit. Process. 11 (1), 87–90. https://doi.org/10.1007/s10339-009-0355-y.

Bullmore, E., Sporns, O., 2009. Complex brain networks: graph theoretical analysis of structural and functional systems. Nat. Rev. Neurosci. 10 (3), 186–198. https://doi.org/10.1038/nrn2575.

Calhoun, V.D., Adali, T., Pearlson, G.D., Pekar, J.J., 2001. A method for making group inferences from functional MRI data using independent component analysis. Hum. Brain Mapp. 14 (3), 140–151. https://doi.org/10.1002/hbm.1048.

Chang, C., Glover, G.H., 2010. Time-frequency dynamics of resting-state brain connectivity measured with fMRI. Neuroimage 50 (1), 81–98. https://doi.org/10.1016/j.neuroimage.2009.12.011.

Chen, P., Xie, Q., Wu, X., Huang, H., et al., 2018. Abnormal effective connectivity of the anterior forebrain regions in disorders of consciousness. Neurosci. Bull. 34 (4), 647–658. https://doi.org/10.1007/s12264-018-0250-6.

Cohen, J.R., D'Esposito, M., 2016. The segregation and integration of distinct brain networks and their relationship to cognition. J. Neurosci. 36 (48), 12083–12094. https://doi.org/10.1523/Jneurosci.2965-15.2016.

Crone, J.S., Soddu, A., Holler, Y., Vanhaudenhuyse, A., Schurz, M., et al., 2014. Altered network properties of the fronto-parietal network and the thalamus in impaired consciousness. NeuroImage Clin. 4, 240–248. https://doi.org/10.1016/j.nicl.2013.12.005.

Damaraju, E., Allen, E.A., Belger, A., Ford, J.M., McEwen, S., et al., 2014. Dynamic functional connectivity analysis reveals transient states of dysconnectivity in schizophrenia. NeuroImage Clin. 5, 298–308. https://doi.org/10.1016/j.nicl.2014.07.003.

Demertzi, A., Antonopoulos, G., Heine, L., Voss, H.U., Crone, J.S., et al., 2015. Intrinsic functional connectivity differentiates minimally conscious from unresponsive patients. Brain 138, 2619–2631. https://doi.org/10.1093/brain/awv169.

Demertzi, A., Gomez, F., Crone, J.S., Vanhaudenhuyse, A., Tshibanda, L., et al., 2014. Multiple fMRI system-level baseline connectivity is disrupted in patients with consciousness alterations. Cortex 52, 35–46. https://doi.org/10.1016/j.cortex.2013.11.005.

Demertzi, A., Tagliazucchi, E., Dehaene, S., Deco, G., Barttfeld, P., et al., 2019. Human consciousness is supported by dynamic complex patterns of brain signal coordination. Sci. Adv. 5 (2). https://doi.org/10.1126/sciadv.aat7603. ARTN eaat7603.

Di, H.B., Yu, S.M., Weng, X.C., Laureys, S., Yu, D., et al., 2007. Cerebral response to patient's own name in the vegetative and minimally conscious states. Neurology 68 (12), 895–899. https://doi.org/10.1212/01.wnl.0000258544.79024.d0.

Perri, Di, C., Bahri, A., M., Amico, E., Thibaut, A., Heine, L., et al., 2016. Neural correlates of consciousness in patients who have emerged from a minimally conscious state: a cross-sectional multimodal imaging study. Lancet Neurol. 15 (8), 830–842. https://doi.org/10.1016/s1474-4422(16)00111-3.

Fernandez-Espejo, D., Soddu, A., Cruse, D., Palacios, E.M., Junque, C., et al., 2012. A role for the default mode network in the bases of disorders of consciousness. Ann. Neurol. 72 (3), 335–343. https://doi.org/10.1002/ana.23635.

Fridman, E.A., Beattie, B.J., Broft, A., Laureys, S., Schiff, N.D., 2014. Regional cerebral metabolic patterns demonstrate the role of anterior forebrain mesocircuit dysfunction in the severely injured brain. Proc. Natl. Acad. Sci. USA 111 (17), 6473–6478. https://doi.org/10.1073/pnas.1320969111.

Friederici, A.D., Chomsky, N., Berwick, R.C., Moro, A., Bolhuis, J.J., 2017. Language, mind and brain. Nat. Hum. Behav. 1 (10), 713–722. https://doi.org/10.1038/s41562-017-0184-4.

Fu, Z., Tu, Y., Di, X., Du, Y., Pearlson, G.D., et al., 2018. Characterizing dynamic amplitude of low-frequency fluctuation and its relationship with dynamic functional connectivity: an application to schizophrenia. Neuroimage 180 (Pt B), 619–631. https://doi.org/10.1016/j.neuroimage.2017.09.035.

Gallen, C.L., Turner, G.R., Adnan, A., D'Esposito, M., 2016. Reconfiguration of brain network architecture to support executive control in aging. Neurobiol. Aging 44, 42–52. https://doi.org/10.1016/j.neurobiolaging.2016.04.003.

Giacino, J.T., Fins, J.J., Laureys, S., Schiff, N.D., 2014. Disorders of consciousness after acquired brain injury: the state of the science. Nat. Rev. Neurol. 10 (2), 99–114. https://doi.org/10.1038/nrneurol.2013.279.

Godwin, D., Barry, R.L., Marois, R., 2015. Breakdown of the brain's functional network modularity with awareness. Proc. Natl. Acad. Sci. USA 112 (12), 3799–3804. https://doi.org/10.1073/pnas.1414466112.

Grady, C., Sarraf, S., Saverino, C., Campbell, K., 2016. Age differences in the functional interactions among the default, frontoparietal control, and dorsal attention networks. Neurobiol. Aging 41, 159–172. https://doi.org/10.1016/j.neurobiolaging.2016.02.020.

Hannawi, Y., 2016. Resting brain activity in disorders of consciousness: a systematic review and meta-analysis (vol 84, pg 1272, 2015). Neurology 86 (2). https://doi.org/10.1212/Wnl.0000000000002301. 202-202.

Kafashan, M., Ching, S., Palanca, B.J., 2016. Sevoflurane alters spatiotemporal functional connectivity motifs that link resting-state networks during wakefulness. Front. Neural Circuits 10, 107. https://doi.org/10.3389/fncir.2016.00107.

Kalmar, K., Giacino, J.T., 2005. The JFK coma recovery scale - revised. Neuropsychol. Rehabil. 15 (3-4), 454–460. https://doi.org/10.1080/09602010443000425.

Kotchoubey, B., Merz, S., Lang, S., Markl, A., Muller, F., et al., 2013. Global functional connectivity reveals highly significant differences between the vegetative and the minimally conscious state. J. Neurol. 260 (4), 975–983. https://doi.org/10.1007/s00415-012-6734-9.

Laureys, S., 2005. The neural correlate of (un)awareness: lessons from the vegetative state. Trends Cognit. Sci. 9 (12), 556–559. https://doi.org/10.1016/j.tics.2005.10.010.

Laureys, S., Faymonville, M.E., Degueldre, C., Fiore, G.D., Damas, P., et al., 2000. Auditory processing in the vegetative state. Brain 123 (Pt 8), 1589–1601.

Li, X., Zhu, D.J., Jiang, X., Jin, C.F., Zhang, X., et al., 2014. Dynamic functional connectomics signatures for characterization and differentiation of PTSD patients. Hum. Brain Mapp. 35 (4), 1761–1778. https://doi.org/10.1002/hbm.22290.

Mashour, G.A., Hudetz, A.G., 2018a. Neural correlates of unconsciousness in large-scale brain networks. Trends Neurosci. 41 (3), 150–160. https://doi.org/10.1016/j.tins.2018.01.003.

Mashour, G.A., Hudetz, A.G., 2018b. Neural correlates of unconsciousness in large-scale brain networks. Trends Neurosci. 41 (3), 150–160. https://doi.org/10.1016/j.tins.2018.01.003.

Monti, M.M., Pickard, J.D., Owen, A.M., 2013. Visual cognition in disorders of consciousness: from V1 to top-down attention. Hum. Brain Mapp. 34 (6), 1245–1253. https://doi.org/10.1002/hbm.21507.

Monti, M.M., Vanhaudenhuyse, A., Coleman, M.R., Boly, M., Pickard, J.D., et al., 2010. Willful modulation of brain activity in disorders of consciousness. N. Engl. J. Med. 362 (7), 579–589. https://doi.org/10.1056/NEJMoa0905370.

Nomura, E.M., Gratton, C., Visser, R.M., Kayser, A., Perez, F., et al., 2010. Double dissociation of two cognitive control networks in patients with focal brain lesions. In: Proceedings of the National Academy of Sciences of the United States of America. 107. pp. 12017–12022. https://doi.org/10.1073/pnas.1002431107.

Ou, J.L., Lian, Z.C., Xie, L., Li, X., Wang, P., et al., 2014. Atomic dynamic functional interaction patterns for characterization of ADHD. Hum. Brain Mapp. 35 (10), 5262–5278. https://doi.org/10.1002/hbm.22548.

Ovadia-Caro, S., Nir, Y., Soddu, A., Ramot, M., Hesselmann, G., et al., 2012. Reduction in inter-hemispheric connectivity in disorders of consciousness. PLoS One 7 (5), e37238. https://doi.org/10.1371/journal.pone.0037238.

Owen, A.M., Coleman, M.R., Boly, M., Davis, M.H., Laureys, S., et al., 2006. Detecting awareness in the vegetative state. Science 313 (5792). https://doi.org/10.1126/science.1130197. 1402.

Owen, A.M., Coleman, M.R., Menon, D.K., Johnsrude, I.S., Rodd, J.M., et al., 2005. Residual auditory function in persistent vegetative state: a combined pet and fMRI study. Neuropsychol. Rehabil. 15 (3-4), 290–306. https://doi.org/10.1080/09602010443000579.

Perri, D., Amico, E., Heine, L., Annen, J., Martial, C., et al., 2018. Multifaceted brain networks reconfiguration in disorders of consciousness uncovered by co-activation patterns. Hum. Brain Mapp. 39 (1), 89–103. https://doi.org/10.1002/hbm.23826.

Preti, M.G., Bolton, T.A., Van De Ville, D., 2017. The dynamic functional connectome: state-of-the-art and perspectives. Neuroimage 160, 41–54. https://doi.org/10.1016/j.neuroimage.2016.12.061.

Qin, J., Chen, S.G., Hu, D.W., Zeng, L.L., Fan, Y.M., et al., 2015. Predicting individual brain maturity using dynamic functional connectivity. Front. Hum. Neurosci. 9https://doi.org/10.3389/fnhum.2015.00418. doi:ARTN 418.

Raichle, M.E., 2015. The restless brain: how intrinsic activity organizes brain function. Philos. Trans. R. Soc. B Biol. Sci. 370 (1668), 82–92. https://doi.org/10.1098/rstb.2014.0172. doi:ARTN 20140172.

Rashid, B., Damaraju, E., Pearlson, G.D., Calhoun, V.D., 2014. Dynamic connectivity states estimated from resting fMRI identify differences among schizophrenia, bipolar disorder, and healthy control subjects. Front. Hum. Neurosci. 8, 897. https://doi.org/10.3389/fnhum.2014.00897.

Rosazza, C., Andronache, A., Sattin, D., Bruzzone, M.G., Marotta, G., et al., 2016. Multimodal study of default-mode network integrity in disorders of consciousness. Ann. Neurol. https://doi.org/10.1002/ana.24634.

Schiff, N.D., 2008. Central thalamic contributions to arousal regulation and neurological disorders of consciousness. Mol. Biophys. Mech. Arousal Alertness Attention 1129, 105–118. https://doi.org/10.1196/annals.1417.029.

Schiff, N.D., 2010. Recovery of consciousness after brain injury: a mesocircuit hypothesis. Trends Neurosci. 33 (1), 1–9. https://doi.org/10.1016/j.tins.2009.11.002.

Schiff, N.D., Giacino, J.T., Kalmar, K., Victor, J.D., Baker, K., et al., 2007. Behavioural improvements with thalamic stimulation after severe traumatic brain injury. Nature 448 (7153), 600–610. https://doi.org/10.1038/nature06041.

Schnakers, C., Vanhaudenhuyse, A., Giacino, J., Ventura, M., Boly, M., et al., 2009. Diagnostic accuracy of the vegetative and minimally conscious state: Clinical consensus versus standardized neurobehavioral assessment. BMC Neurol. 9https://doi.org/10.1186/1471-2377-9-35. doi:Artn 35.

Shen, X., Finn, E.S., Scheinost, D., Rosenberg, M.D., Chun, M.M., et al., 2017. Using connectome-based predictive modeling to predict individual behavior from brain connectivity. Nat. Protoc. 12 (3), 506–518. https://doi.org/10.1038/nprot.2016.178.

Siegel, J.S., Ramsey, L.E., Snyder, A.Z., Metcalf, N.V., Chacko, R.V., et al., 2016. Disruptions of network connectivity predict impairment in multiple behavioral domains after stroke. Proc. Natl. Acad. Sci. USA 113 (30), E4367–E4376. https://doi.org/10.1073/pnas.1521083113.

Song, M., Yang, Y., He, J.H., Yang, Z.Y., Yu, S., et al., 2018. Prognostication of chronic disorders of consciousness using brain functional networks and clinical characteristics. Elife 7https://doi.org/10.7554/eLife.36173. doi:ARTN e36173.

Tagliazucchi, E., Laufs, H., 2014. Decoding wakefulness levels from typical fMRI resting-state data reveals reliable drifts between wakefulness and sleep. Neuron 82 (3), 695–708. https://doi.org/10.1016/j.neuron.2014.03.020.

Tomasi, D., Volkow, N.D., 2018. Association between brain activation and functional connectivity. Cereb. Cortex. https://doi.org/10.1093/cercor/bhy077.

van den Heuvel, M.P., Sporns, O., 2019. A cross-disorder connectome landscape of brain dysconnectivity. Nat. Rev. Neurosci. https://doi.org/10.1038/s41583-019-0177-6.

Vanhaudenhuyse, A., Noirhomme, Q., Tshibanda, L.J., Bruno, M.A., Boveroux, P., et al., 2010. Default network connectivity reflects the level of consciousness in non-communicative brain-damaged patients. Brain 133 (Pt 1), 161–171. https://doi.org/10.1093/brain/awp313.

Vidaurre, D., Abeysuriya, R., Becker, R., Quinn, A.J., Alfaro-Almagro, F., et al., 2018. Discovering dynamic brain networks from big data in rest and task. Neuroimage 180 (Pt B), 646–656. https://doi.org/10.1016/j.neuroimage.2017.06.077.

Vidaurre, D., Smith, S.M., Woolrich, M.W., 2017. Brain network dynamics are hierarchically organized in time. Proc. Natl. Acad. Sci. USA 114 (48), 12827–12832. https://doi.org/10.1073/pnas.1705120114.

Weng, L., Xie, Q., Zhao, L., Zhang, R., Ma, Q., et al., 2017. Abnormal structural connectivity between the basal ganglia, thalamus, and frontal cortex in patients with disorders of consciousness. Cortex 90, 71–87. https://doi.org/10.1016/j.cortex.2017.02.011.

Wijdicks, E.F.M., 2018. Who improves from coma, how do they improve, and then what? Nat. Rev. Neurol. 14 (12), 694–697. https://doi.org/10.1038/s41582-018-0084-x.

Wise, R.J.S., Scott, S.K., Blank, S.C., Mummery, C.J., Murphy, K., et al., 2001. Separate neural subsystems within 'Wernicke's area'. Brain 124, 83–95. https://doi.org/10.1093/brain/124.1.83.

Yao, S., Song, J., Gao, L., Yan, Y., Huang, C., et al., 2015. Thalamocortical sensorimotor circuit damage associated with disorders of consciousness for diffuse axonal injury patients. J. Neurol. Sci. 356 (1-2), 168–174. https://doi.org/10.1016/j.jns.2015.06.044.

Zhu, J., Wu, X., Gao, L., Mao, Y., Zhong, P., et al., 2009. Cortical activity after emotional visual stimulation in minimally conscious state patients. J. Neurotrauma 26 (5), 677–688. https://doi.org/10.1089/neu.2008.0691.